Arabian Journal of Chemistry (2022) **15**, 104172

King Saud University

Arabian Journal of Chemistry

www.ksu.edu.sa
www.sciencedirect.com

ORIGINAL ARTICLE

Proton conducting polymer blend electrolytes based on MC: FTIR, ion transport and electrochemical studies

Jihad M. Hadi [a], Shujahadeen B. Aziz [b,c,*], Hwda Ghafur Rauf [d], Rebar T. Abdulwahid [b,e], Sameerah I. Al-Saeedi [f], Dana A. Tahir [g], M.F.Z. Kadir [h]

[a] *Nursing Department, College of Nursing, University of Human Development, Kurdistan Regional Government, Iraq*
[b] *Hameed Majid Advanced Polymeric Materials Research Lab., Physics Department, College of Science, University of Sulaimani, Qlyasan Street, Sulaimani 46001, Kurdistan Regional Government, Iraq*
[c] *The Development Center for Research and Training (DCRT), University of Human Development, Sulaymaniyah, Kurdistan Region of Iraq, Iraq*
[d] *Department of Medical Laboratory Science, College of Science, Komar University of Science and Technology, Sulaimani 46001, Kurdistan Regional Government, Iraq*
[e] *Department of Physics, College of Education, University of Sulaimani, Old Campus, Sulaymaniyah 46001, Iraq*
[f] *Department of Chemistry, College of Science, Princess Nourah bint Abdulrahman University, P.O.Box 84428, Riyadh 11671, Saudi Arabia*
[g] *Department of Physics, College of Science, University of Halabja, Halabja 46006, Kurdistan Regional Government, Iraq*
[h] *Physics Department, Faculty of Science, Universiti Malaya, 50603 Kuala Lumpur, Malaysia*

Received 2 April 2022; accepted 4 August 2022
Available online 12 August 2022

KEYWORDS

Polymer blends;
Ammonium salt;
FTIR study;
EIS and EEC modeling;
TNM and LSV

Abstract In this work, the free-standing plasticized solid polymer electrolyte films were made utilizing methylcellulose (MC) and dextran (DN) doped with ammonium fluoride (NH_4F) and plasticized with glycerol by a typical solution casting approach. Based on the characterizations, MC-DN-NH_4F electrolyte has been shown to improve the structural, electrical, and electrochemical properties resulting from the dispersion of glycerol plasticizer. The electrochemical impedance spectroscopy (EIS) measurement for the highest inclusion of plasticizer revealed a conductivity of 2.25×10^{-3} S/cm. The electrical equivalent circuit (EEC) model has established the circuit elements for each electrolyte. The variation trend of dielectric constant and DC conductivity was matched and confirmed by the EIS data. The fourier transform infrared (FTIR) analysis displayed credible

* Corresponding author.
E-mail address: shujahadeenaziz@gmail.com (S.B. Aziz).
Peer review under responsibility of King Saud University.

Production and hosting by Elsevier

https://doi.org/10.1016/j.arabjc.2022.104172

confirmation of polymers-ion-plasticizer interactions. The dielectric study is extra highlighted the conductivity behavior. The dielectric constant and loss (ε′ and ε″) quantities were reported to be high at low frequencies. On the other hand, the irregular shape of the imaginary part of modulus (M‘‘) spectra denotes the non-Debye behaviors of relaxation. The ion transference number (t_{ion}) value for the maximum plasticized system is 0.944, where the ions are the primary components for the charge transfer process. Stability of the highest conducting sample is determined to be 1.6 V, using linear sweep voltammetry (LSV).

1. Introduction

Electrochemical capacitors (ECs), also known as supercapacitors (SCs), are now being studied extensively due to their unique properties in terms of energy and power densities. ECs are electrical devices that can accumulate and share out charges in an extremely reversible manner (Yang et al., 2010). For decades, SCs have been employed in a diversity of applications including, common household electronics, vehicles, medical devices, and defense-related systems (Kumar et al., 2012). Unlike batteries, supercapacitors offer a very much longer service life and high cycling capabilities without sacrificing energy storage capacity. SCs are available in two configurations; symmetric (electrodes have the same capacitance) and asymmetric (electrodes with varying capacitance). Whereas, an asymmetric capacitor may possess a pair of separate pseudocapacitive electrodes or a double-layer electrode plus pseudocapacitive electrode (Gao and Lian, 2014). SCs are categorize according to their charge storage mechanism. It can be divided into pseudo capacitors (PCs), hybrid capacitors (HCs), and electrical double-layer capacitors (EDLCs). Pseudo capacitor stores energy by transferring charge between electrolyte and electrodes through Faradaic mechanisms while (EDLC) stores energy electrostatically at the interfaces between electrolyte and electrodes as charge separation using non-Faradaic mechanisms. However, (HCs) combine (PCs) and (EDLCs) methods (Nofal et al., 2020; Iro et al., 2016; Kiamahalleh et al., 2012).

Polymer electrolytes (PEs) have gotten a lot of interest since they could be used in electrochemical devices. It has a lot of compensation, including strong mechanical qualities, the capability to create appropriate electrode–electrolyte interactions, and its ease to film fabrication. These features make it possible to be employed in a variety of electrochemical device applications (Ahmed and Abdullah, 2020; Khiar et al., 2006). The majority widespread polymer electrolytes consist of neutral polar polymers, which it is complex with alkali metal salts, including ammonium and lithium salts, divalent transition metals, and acids. The key commonly researched biopolymer electrolytes are cellulose and its derivatives (Shuhaimi et al., 2012; Dueramae et al., 2020), chitosan (Hadi et al., 2020), dextran (Hamsan et al., 2019), and starch (Shukur et al., 2013). A methylcellulose (MC) is a water-soluble biopolymer made up of β (1–4) glycosidic units in its linear chain and substituting with a methyl group. MC possesses a variety of exceptional properties for instance non-toxic, low-cost, and oxygen-containing atoms with electron pairs that allow salt cations to interact with the polymer in a loose manner. These properties provide inspiration for research on methylcellulose-based polymer electrolytes (Nofal et al., 2021; Shuhaimi et al., 2010). On the other hand, dextran (DN) ensures the ability to operate as an ionic conductor by the presence of two important functional groups (–OH) and glycosidic bonds. It is attained from *Leuconostoc mesenteroides* bacterial cultures (Hamsan et al., 2020; Dumitraşcu et al., 2012). In this study, a simple technique of polymer blend has been used in which two or more polymers are combined to generate a better material. This is due to the functional groups of each polymer interacting with one another, providing additional ion routes (Aziz et al., 2021). Recent studies have shown that biodegradable polymer electrolytes have the potential to be used in energy conversion devices. Our earlier studies for the MC-DN blend polymers proved their suites in the development of high-performance electrochemical devices (Hadi et al., 2022; Aziz et al., 2022). In particular, methylcellulose-based electrolytes possess a relatively high energy density which is almost close enough to lead-acid batteries (Aziz et al., 2022).

Many ionic sources could be used in solid polymer electrolyte applications like potassium, sodium, lithium, silver, and ammonium salts. Ammonium fluoride (NH_4F) has been employed in the construction of proton conducting MC-DN polymer mix electrolytes in this study. Since ammonium salts have excellent ionic conductivity, compatibility with other elements, and thermal stability, they have been studied as a possible source of a proton (H^+). Inorganic acids can also provide proton (H^+) like phosphoric acid (H_3PO_4) and sulfuric acid (H_2SO_4) while their chemical breakdown is not beneficial for energy storage applications (Prajapati et al., 2010; Asnawi et al., 2020; Hamsan et al., 2020). The NH_4F salt has been shown to increase the ionic conductivity of an electrolyte system by up to 10^{-3} S/cm as reported by Hamsan et al. (Ikmar Nizam Mohamad Isa et al., 2014). Furthermore, it has also been noted that adding NH_4F salt enhanced the ionic conductivity for the carboxymethylcellulose (CMC) based polymer electrolytes, as reported by M. A. Ramli and M.I.N Isa (Aziz et al., 2021). It was proven that the ionic conductivity is enhanced in the plasticization methodology by providing more pathways for ions to move comfortably, resulting in high salt dissociations. There has been numerous research published in the literature that has generated polymer electrolytes with varied glycerol contents (Chai and Isa, 2016; Mustafa et al., 2020; Hadi et al., 2020). Lately, sophisticated models for calculating ion transport parameters based on EIS and dielectric relaxation theories were reported (Nofal et al., 2021; Shuhaimi et al., 2010; Aziz et al., 2022). Thereby, in this study, the influence of various glycerol concentrations on ion transport properties of the MC-DN-NH_4F-based polymer electrolyte will be investigated. Then, the eligibility of the prepared polymer based electrolyte for energy device application will be explored using various electrochemical analysis techniques.

2. Experimental details

2.1. Raw materials and sample preparation

As provided by Sigma-Aldrich (Kuala Lumpur, Malaysia) and to fabricate the electrolytes, methylcellulose (MC), dextran (DN), ammonium fluoride (NH_4F), and low molecular weight of glycerol plasticizer were used. At ambient temperature, each of 40 wt% of DN (0.4 g) and 60 wt% of MC (0.6 g) were dissolved in two different containers in a 1 % solution of acetic acid (50 mL) for about 2 h to synthesize the MC-DN blend polymer. Later, by dissolving a specific amount of NH_4F (40 wt%), polymer electrolytes based on MC-DN-NH_4F were obtained. Following that, the solutions were mixed and stirred for approximately 4 h with a magnetic stirrer to achieve a homogeneous solution. After that, glycerol was gradually

added to the MC-DN-NH_4F mixture, with varying the quantities from 14 to 42 wt% in steps of 14 wt% during continuous stirring, which to yielded plasticized solid polymer electrolytes. The MC-DN-NH_4F electrolytes containing 14, 28, and 42 wt % of glycerol were coded as PBGF1, PBGF2, and PBGF3, respectively. After that, the whole electrolytes were left at room temperature in the designated Petri dishes for slow evaporation, so the solution casting process was carried out. Finally, the dried films were put into a desiccator to ensure complete evaporation.

2.2. Characterization techniques

The FTIR spectra ranging from 500 to 4000 cm^{-1} with a resolution of 1 cm^{-1} were obtained using Spotlight 400 spectrometer (Perkin Elmer, Waltham, MA, USA) to established the synthesis of the plasticized polymer blend electrolyte. Using a 3532–50 LCR HiTESTER (HIOKI, Nagano, Japan), electrochemical impedance spectroscopy (EIS) was utilized to investigate the materials' electrochemical characteristics. The thickness of the electrolytes was installed between a pair of stainless-steel (SS) electrodes and set at 150–152 μA. After connecting the cell to a computer, it was programmed to derive the complex (Z*) impedance spectroscopy's real (Z') and imaginary (Z'') components. Using a polarized SS/uppermost conducting electrolyte/SS cell and a voltage of 0.2 V, transference number measurement (TNM) computed the ion and electron transference numbers (t_{ion} and t_{el}). To determine the sample's transport numbers, a DP 3003 Digital DC power supply was used at room temperature (V & A instrument, Shanghai, China). A Digi-IVY DY2300 potentiostat was used for linear sweep voltammetry (LSV) to determine the highest conducting system maximum working potential. TNM and the cell layout were accurately matched.

3. Results and discussion

3.1. Impedance analysis

EIS is a widespread device for evaluating the ionic conductivity and electrical characteristics of original materials in electrochemical device applications. Because of their wide range of uses as energy storage devices, ion conducting materials have received much interest in recent years. A semicircle and a spike in polymer electrolytes impedance responses at high and low frequencies, respectively, are common observations. Fig. 1 demonstrates the impedance plot (Z_i vs Z_r) for the MC-DN-NH_4F containing various concentrations of glycerol (Awasthi and Das, 2019).

As an EIS was examined, a simple electrical equivalent circuit (EEC) model was chosen since it provides a clear image of the system. Usually, EEC is composed of a constant phase element (CPE) comprising bulk resistance (R_b) for the charge carriers. Impedance spectrums for circuits containing capacitors and resistors in parallel must be semicircle in shape, with a diameter that corresponds to the real axis. Because there is no semicircle at higher frequencies, ions are most likely responsible for conduction, according to the findings in this study. At the blocking electrodes, an electrical double-layer capacitance causes a linear line to appear at low frequencies. It is noteworthy that the glycerol plasticizer is responsible for the absence of semicircles at high frequencies, as shown in Fig. 1 (a-c). The impedance of CPE (Z_{CPE}) is calculated using the following relation (Aziz et al., 2021; Aziz et al., 2020; Malathi et al., 2010):

$$Z_{CPE} = \frac{1}{C\omega^p}\left[cos\left(\frac{\pi p}{2}\right) - isin\left(\frac{\pi p}{2}\right)\right] \quad (1)$$

Where C stands for the capacitance, ω denotes the angular frequency, and P represents the plots' deviation measure. CPE is linked in series with the bulk resistance of samples in our study, and their EIS responses show simply the spike. The following equation, which contains only a spike, can be used to represent the real (Z') and imaginary (Z'') components of impedance:

$$Z' = R_b + \frac{\cos\left(\frac{\pi p}{2}\right)}{C\omega^p} \quad (2)$$

$$Z'' = \frac{\sin\left(\frac{\pi p}{2}\right)}{C\omega^p} \quad (3)$$

Table 1 lists the P and CPE values for the MC-DN-NH_4F containing various glycerol content. The rise in free ion number in the electrolyte systems may explain the elevated CPE levels with the increment of glycerol. Consequently, the electrode polarization (EP) acceleration increases, resulting in a higher capacitance value at low frequencies. Therefore, the insertion of glycerol supports salt dissociation and increases ionic mobility.

It is crucial to apply the following equation to obtain the (σ_{dc} σ_{dc}) ionic conductivity for the MC-DN-NH_4F containing different glycerol concentrations based on the (R_b) value (Maheshwari et al., 2021; Hadi et al., 2020; Nik Aziz et al., 2010):

$$\sigma_{dc} = \left[\frac{1}{R_b}\right] \times \left[\frac{t}{A}\right] \quad (4)$$

Where t stands for the thickness of the sample, and A denotes the area of the electrode. The (σ_{dc}) ionic conductivity values for the MC-DN-NH_4F-glycerol systems are summarized in Table 2. It has been shown that rising the glycerol plasticizer from 14 to 42 wt% enhances the (σ_{dc}) from 1.62×10^{-4} S/cm to 2.65×10^{-3} S/cm. The glycerol ratio is vital in improving the electrolyte's ionic conductivity (see Table 2) (Brza et al., 2021). The conductivity is governed by two factors a number of charge carriers and ionic movements. In this study, a charge carrier density of 42 wt% of glycerol was found to be optimal. The relationship between (σ_{dc}) of the electrolytes and ions mobility and ions density is well-understood and represented as follows:

$$\sigma = \sum \eta q\mu \quad (5)$$

Where, (η) denotes the density of the charge carriers, q stands for the simple charge, and the mobility of the ions is denoted by (μ). As predicted, a rise in both η and μ in the electrolytes improves ionic conductivity.

Many equations are used in this study to calculate transport parameters from impedance data that only contained a spike, such as (η), diffusion coefficient (D), and (μ). Here are the formulae that were used to compute the D:

$$D = D_o exp\left\{-0.0297[lnD_o]^2 - 1.4348lnD_o - 14.504\right\} \quad (6)$$

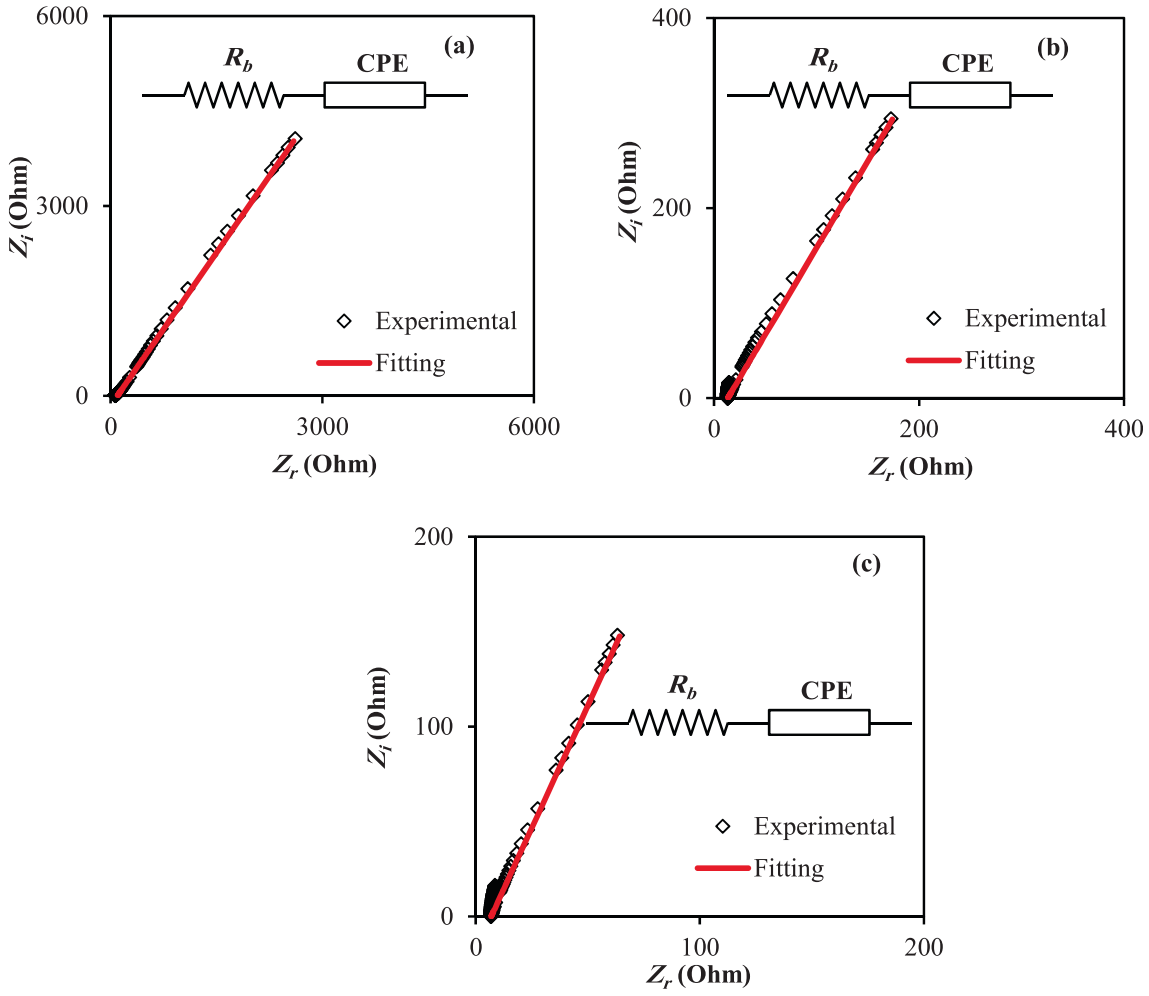

Fig. 1 Impedance spectroscopy plots for the MC-DN-NH_4F containing different glycerol concentrations (a) PBGF1, (b) PBGF2, and (c) PBGF3.

Table 1 The *P* and CPE values for the MC-DN-NH_4F containing various glycerol concentrations.

Sample code	p1	k1	CPE1
PBGF1	0.53	173,800	5.75×10^{-6}
PBGF2	0.48	14,900	6.71×10^{-5}
PBGF3	0.36	11,200	8.93×10^{-5}

Table 2 Impact of glycerol content in MC-DN-NH_4F samples on ionic conductivity and transport parameters values.

Sample code	σ_{dc}	*D*	μ	*n*
PBGF1	1.62×10^{-4}	2.69×10^{-9}	1.05×10^{-7}	9.67×10^{21}
PBGF2	1.15×10^{-3}	1.97×10^{-7}	7.66×10^{-6}	9.34×10^{20}
PBGF3	2.25×10^{-3}	9.88×10^{-7}	3.85×10^{-5}	3.65×10^{20}

$$D_o = \left(\frac{4k^2l^2}{R_b{}^4\omega_{min}{}^3}\right) \tag{7}$$

Where the thickness of the electrolyte is represented by (*l*), and the angular frequency at the minimum (Z_i) value is denoted by (ω_{min}). In addition, equation (8) is utilized to compute ionic mobility (Turhan et al., 2001):

$$\mu = \left(\frac{eD}{K_bT}\right) \tag{8}$$

Here, the Boltzmann constant is indicated by (K_b) while the absolute temperature is represented by (*T*). Since the (σ_{dc}) is known, the equation (5) can be used to compute the ions density (η). It can be noticed that the value of D increased considerably with increasing glycerol concentrations from 14 to 28 wt % (see Table 2). It is also observed that a comparable tendency is followed for ionic mobility. Glycerol plasticizer encourages chain flexibility, which results in an increase in the ionic conductivity. Due to the presence of glycerol, salts are more likely to be dissociated into free ions (Hadi et al., 2020).

3.2. FTIR study

The FTIR method was used to analyze the engagement between ions and atoms in the PBGF electrolyte systems. Fig. 2 depicts the FTIR spectra for the MC-DN-NH_4F con-

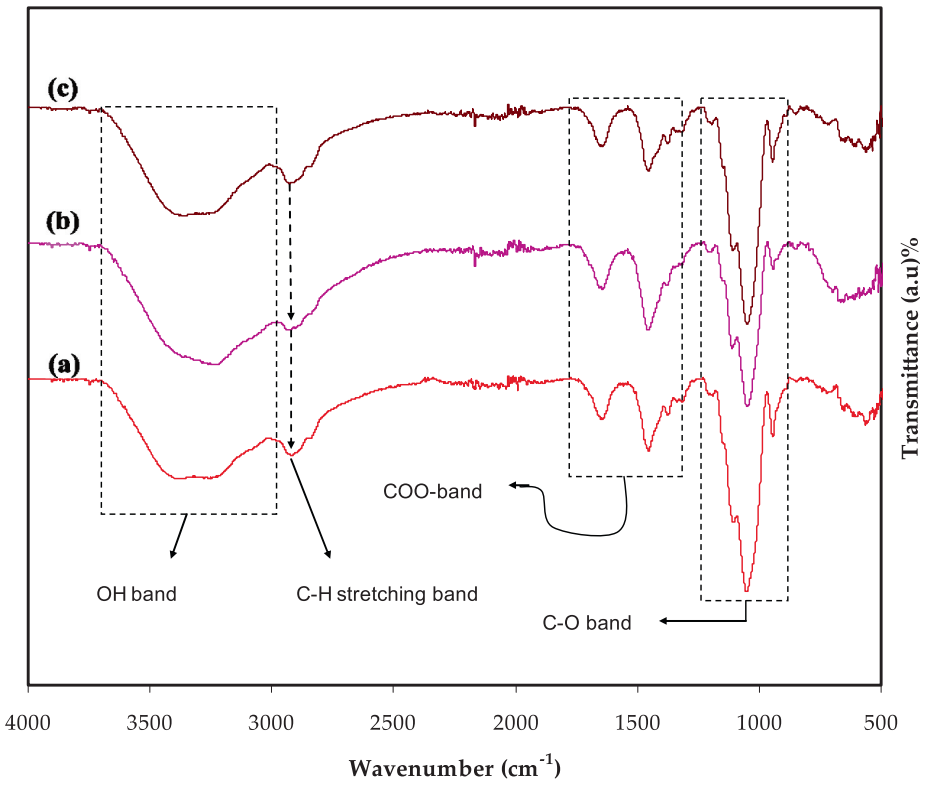

Fig. 2 FTIR spectra for the MC-DN-NH_4F containing various glycerol concentrations (a) PBGF1, (b) PBGF2, and (c) PBGF3.

taining different glycerol concentrations. Infrared spectroscopy shows development in the hydrogen bond in the electrolyte samples where the hydrogen bond affects the stretching vibrations (Nofal et al., 2021). A broad peak appearing at a wavenumber of ~ 3400 cm^{-1} for each is corresponding to the (O—H) band of the polymers, and the ether band is linked to the peak appearing at ~ 1050 cm^{-1}. Approximately peaks at around 1480 cm^{-1} and 1640 cm^{-1}, are measured for (COO–) symmetric stretching and asymmetric stretching, as well as (C—H) aliphatic, respectively. (Abdulwahid et al., 2022; Vettori et al., 2012; Shigel, 2002). A peak was observed at about 1040 cm^{-1} is connected to the C—O band in ether, as shown in Fig. 2. The (C—H) stretching modes of the DN can be seen at ~ 2900 cm^{-1}. The covalent vibration and glycosidic bridge of the (C—O—C) band cause to appearing a peek at ~ 920 cm^{-1}, proving the glycosidic bond. The NH^{4+} ion has derived from the NH_4F in conjugation with the oxygen atoms of the (O—H) and (C—O—C) in the blended polymers. Furthermore, the protonation of the electrolyte systems is enhanced by these functional group interactions of (–NH2, C—O in ether, –OH) (Nofal et al., 2022; Deraman et al., 2014). Previous studies have shown that the irregular peaks and variations in the functional group intensities could be utilized to identify the interactions between electrolyte components. In this work, the inclusion of glycerol as a plasticizer causes to dissociation of more salts into free ions, resulting in changes in the band intensities. It is worth noting that changes in band intensity are highly linked to changes in macromolecular arrangements (Aziz et al., 2020). The acquired result is regarded as solid evidence of complexation and excellent miscibility, which are crucial in the production of polymer electrolyte systems.

3.3. Dielectric properties

It has been established previously that dielectric parameters could be used to estimate the ionic transport mechanism and ionic conductivity behavior of polymers-based electrolytes. The frequency-dependent changes in dielectric constant (ε′) and dielectric loss (ε″) are shown in Figs. 3 and 4, which measure the amount of charge stored and energy loss during the movement of ions, respectively. Fig. 3 illustrates the instability in frequency with a dielectric constant for the MC-DN-NH_4F containing different glycerol concentrations (Basha et al., 2018; Dannoun et al., 2022). It can be seen that the dielectric constant drops with increasing frequency, attributed to the ion drifting. It is observed to be high for the sample comprising 42 wt% glycerol concentrations (PBGF3), resulting in high ionic conductivity, and electrode polarization. This indicated that the NH_4F salt has entirely dissolved in the MC-DN blend polymer chains, resulting in ion mobility. At the electrode–electrolyte interface, the forming of the space charge area causes to observe a fluctuation in the dielectric constant with frequency, suggesting non-Debye behavior (Pritam et al., 2020). After extracting (Z' and Z'') from the EIS data, by using the following equations, we are then able to determine (ε′ and ε″) (Arya and Sharma, 2018; Rauf et al., 2022; Aziz et al., 2021; Smaoui et al., 2009):

$$\varepsilon' = \frac{Z''}{C_o\omega\left(Z'^2 + Z''^2\right)} \tag{9}$$

$$\varepsilon'' = \frac{Z'}{C_o\omega\left(Z'^2 + Z''^2\right)} \tag{10}$$

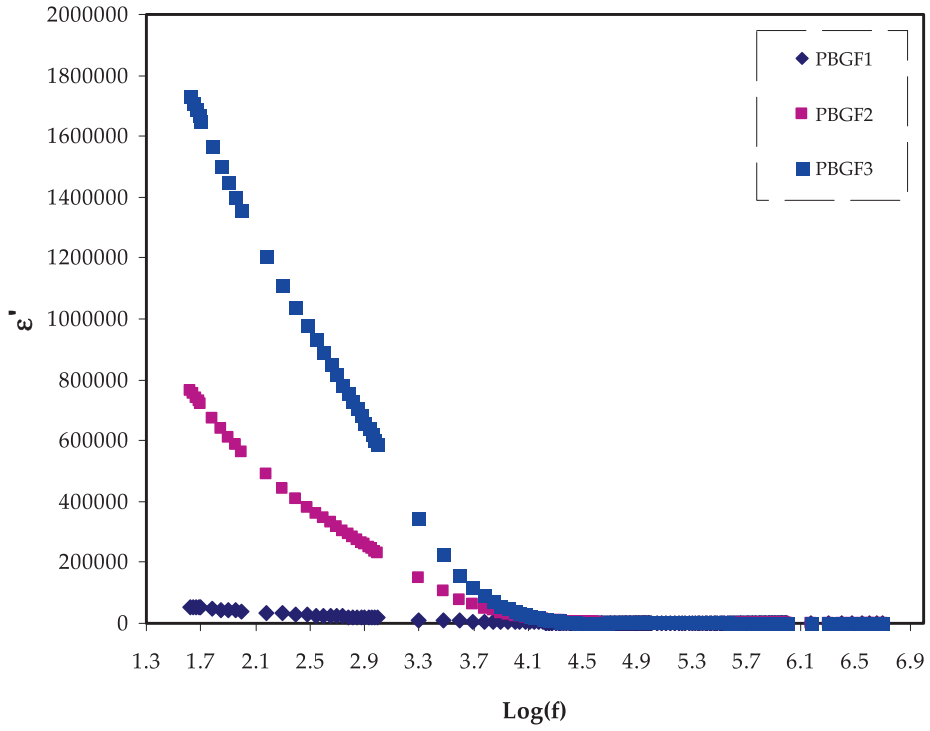

Fig. 3 The ε′ trends for the PBGF samples in the studied frequency range.

Where ω represents the angular frequency, and C_o denotes the capacitance, which are given by ($\omega = 2\pi f$) and $\varepsilon_o A/t$, respectively. In the regions of low frequencies, both the (ε′ and ε″) were observed to be improved with rising plasticizer content. The absence of clear dielectric relaxation peak in Fig. 4 indicates that polymer segmental relaxation is mostly responsible for the ionic conductivity in the systems. However, the increasing frequency causes to decline in the (ε′ and ε″) values and followed by unchanged, ascribing to the electrical field's periodic reversal that happened rapidly among the electrodes (Arya and Sharma, 2018). The impact of glycerol content on the (ε′ and ε″) values in electrolytes has been shown by the dielectric plots, where the treatment of glycerol supports in improving these properties, which are also constituents with conductivity trend. Furthermore, the non-Debye character is also appropriate for explaining the conductivity behavior of electrolytes (Brza et al., 2021).

The reciprocal of the complex relative permittivity is the complex electric modulus (M*), which is crucial for studying the dielectric characteristic of materials, predominantly at low frequencies. Transformed real (M') and imaginary (M'') components of (M*) were used to get electric modulus formalism. The (Z' and Z'') of (M*) were obtained from the EIS data and applied to determine the (M') and (M'') via the following relations (Agrawal et al., 2009; Nofal et al., 2022; Aziz, 2016; Castillo et al., 2009):

$$M' = \frac{\varepsilon'}{(\varepsilon'^2 + \varepsilon''^2)} = \omega C_o Z'' \tag{11}$$

$$M'' = \frac{\varepsilon''}{(\varepsilon'^2 + \varepsilon''^2)} = \omega C_o Z' \tag{12}$$

Figs. 5 and 6 display the real (M') and imaginary (M'') parts against frequency for all PBGF samples at room temperature. At low frequencies, the (M') and (M'') values move toward zero, representing that the electrode polarization (EP) has a insignificant effect on these parameters. The longer tails in low frequencies in *M'* and *M''* figures are due to high electrode capacitance. On the other hand, the (M') values climb with increasing frequency, and the greatest (M') value is reached at a high frequency. This might be due to the fact that the relaxation process takes place at different frequencies. The disappearance of various peaks in (M'') spectra might be related to the frequency limitation of the LCR meter. No equivalent characteristic peaks in the (ε″) spectra (Fig. 4) suggest that the samples have varying relaxation times with varying glycerol contents (Dave and Kanchan, 2018). Therefore, the carriers are saturated in potential and may travel over distance at high frequencies. The absence or development of peaks in the imaginary EIS diagram is related to the effects of space charge and non-localized conductivity. To recognize the conductivity behavior of the films, the (M*) spectrum is promising. Because of the reduction in the effect of (EP) and ionic mobility, highest conducting system moves to beneath of the curves in *M'* and *M''* patterns (Aziz et al., 2010; Shukur and Kadir, 2015).

3.4. Transference number measurement (TNM)

A DC polarization technique (TNM) was used at room temperature to investigate the impact of ionic diffusion on the system's conductivity performance (Aniskari and Mohd Ikmar, 2017) using a V&A Instrument DP3003 digital dc power supply (Chai et al., 2013). Fig. 7 depicts the DC polarization curve of current in the study of time for the uppermost conducting

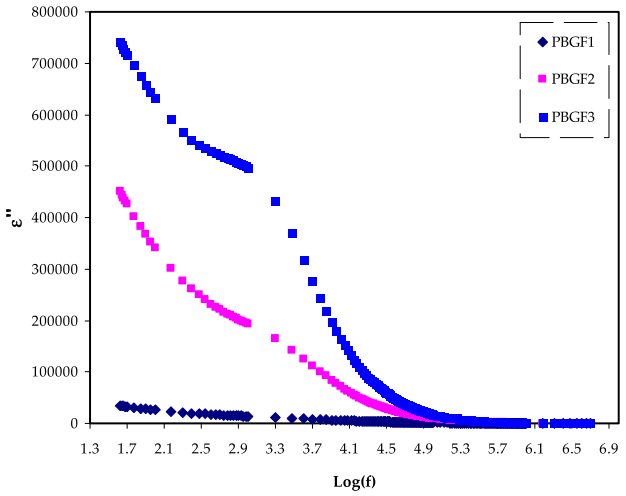

Fig. 4 The ε'' trends for the PBGF samples in the studied frequency range.

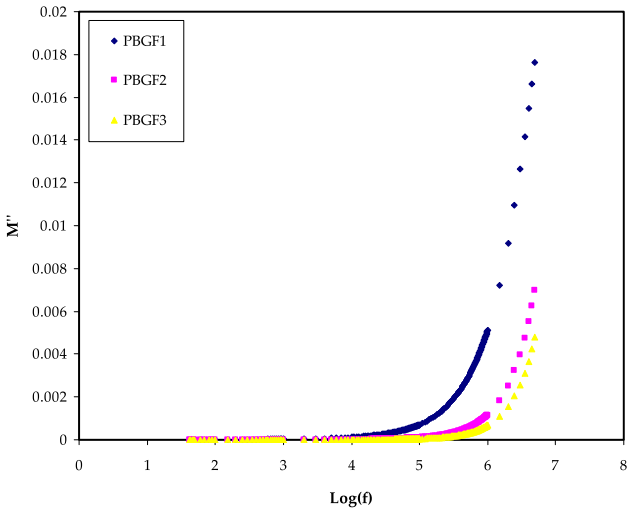

Fig. 6 The M'' trends for the PBGF samples in the studied frequency range.

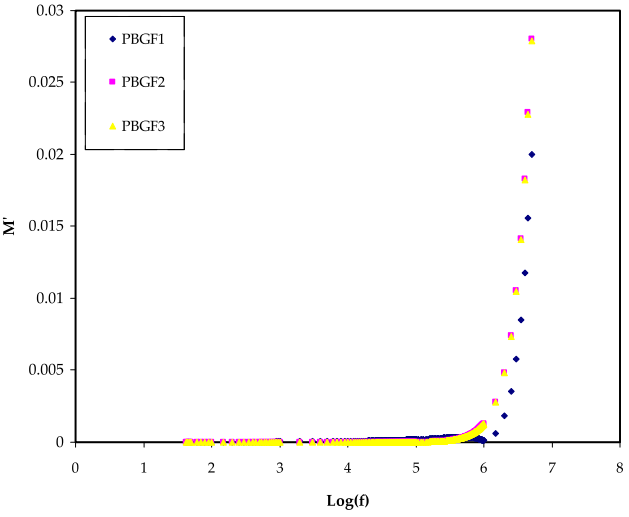

Fig. 5 The M' trends for the PBGF samples in the studied frequency range.

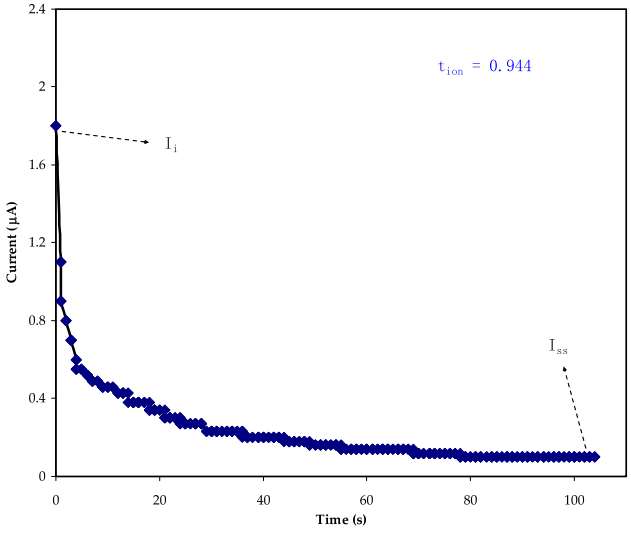

Fig. 7 The DC polarization curve of current in the studied of time for the PBGF3 sample.

electrolyte. Ionic transference number was calculated using a graph of time-dependent normalized polarization current, through applying a steady 0.2 V DC voltage across a sample placed between two stainless steel electrodes (Sohaimy and Isa, 2017). Equations (13) and (14) were utilized to estimate the transport ion (t_{ion}) and transport electrons (t_{el}) of the PBGF3 sample:

$$t_{ion} = \frac{I_i - I_{ss}}{I_i} \tag{13}$$

$$t_{ion} = 1 - t_{el} \tag{14}$$

Where, I_i represents the initial current, and I_{ss} represents the steady-state of the normalized polarization current (Chai et al., 2013). Due to the mainly ionic nature of the electrolyte, the initial total current declines dramatically over time when a voltage is given to the cell, until the cell reaches a stable state at which the cell is polarized due to ionic movements. Moreover, the electronic movement causes the residual current to flow through the electrolyte. In the end, for the highest conductivity sample, the transference numbers resulted to be 0.944, which demonstrates the general cationic nature of conduction species (Hadi et al., 2021; Aziz et al., 2021). Comparable outcomes were obtained for previous works based on the biopolymer electrolytes (Aziz et al., 2021; Ramlli and Isa, 2016; Yusof, 2014). Ramlli and Isa (Li, 2017) have recognized the t_{ion} value of 0.7 for their biopolymer electrolyte system using NH_4F salt as an ionic source.

3.5. Linear sweep voltammetry (LSV)

One of the most helpful decisive factors to evaluate a prepared polymer electrolyte for device application is the electrolyte's

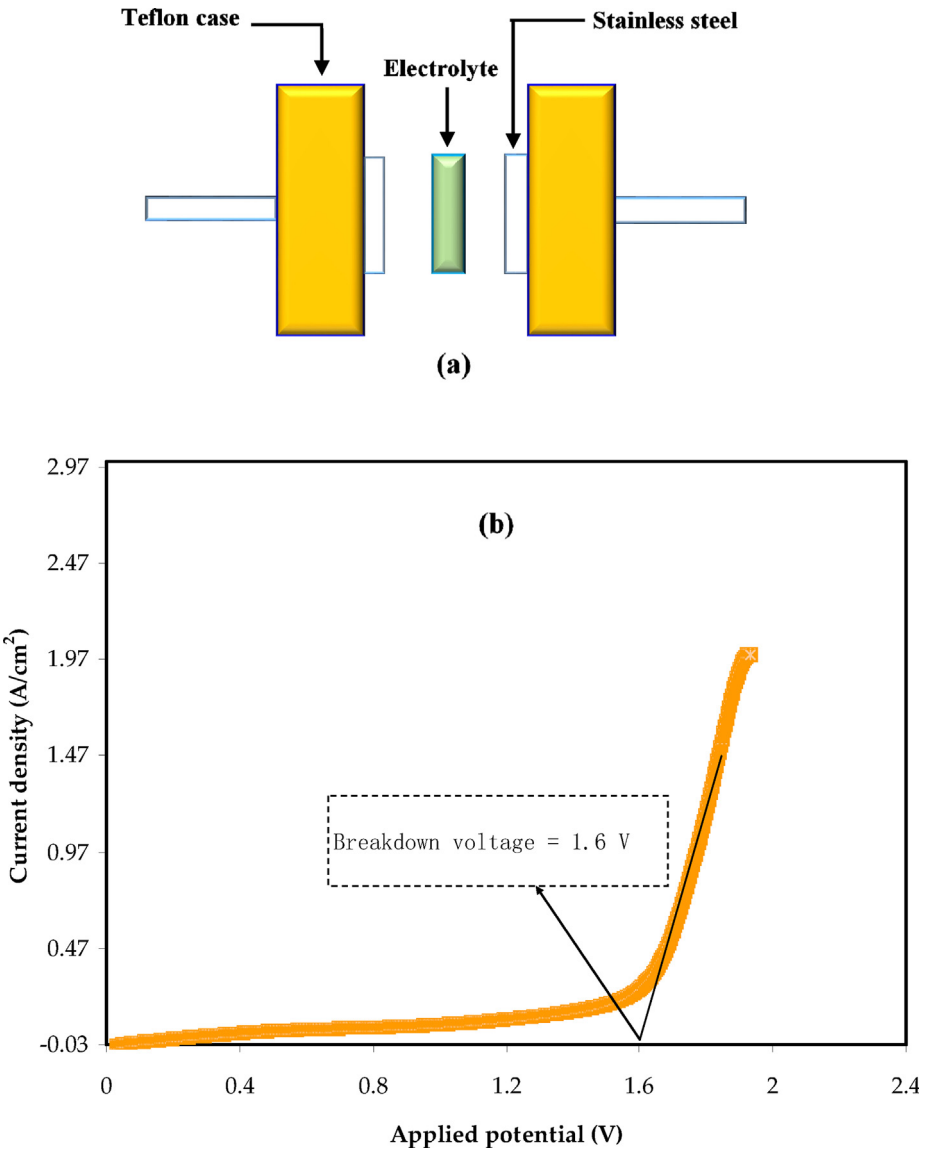

Fig. 8 **(a)** LSV measurement configuration. **(b)** LSV plot for the PBGF3 sample at room temperature.

electrochemical stability and its membrane acceptance toward the applied voltage (Kadir et al., 2018; Rani et al., 2014). Linear sweep voltammetry (LSV) measurement was carried out by utilizing a three-electrode configuration as shown in Fig. 8 **(a)**. As reference electrodes, stainless steel electrodes were employed (Aziz et al., 2021). Fig. 8 (b) depicts the LSV plot for the PBGF3 sample at a working voltage of 10 mV/s. The breakdown voltage of the polymer electrolyte is around 1.6 V at ambient temperature, according to the LSV result. The breakdown voltage of the electrolyte is assumed to occur at the onset current. At electrode potentials above 1.6 V, the current develops gradually. This system's electrochemical window standard is around 1 V, which means that the current system can be used for the production of electrochemical devices [71]. The current is starts to escalate progressively when the breakdown voltage is lower than electrode potential (Aziz et al., 2021). Our previous work for the same blend of polymer-based electrolytes [72] using ammonium thiocyanate (NH_4SCN) salt as an ionic source displayed the LSV value of 2 V. The low lattice energy of NH_4SCN in comparison to NH_4F could explain the high decomposition voltage.

4. Conclusion

In conclusion, three films of solid polymer electrolytes based on MC-DN-NH_4F-glycerol were made using a solution casting process. The impedance and FTIR methods demonstrate that the highest amounts of plasticization have optimal compatibility with the whole electrolytes. As determined by EIS spectroscopy, the PBGF3 sample had a maximum ionic conductivity of 2.25×10^{-3} S/cm. Also, the transport parameters were found to be improved as the inclusion of glycerol increased to the system. It was discovered that the significant dielectric values are due to electrode polarization caused by ion movements. The ion dominancy as a charge carrier has been verified by both TNM and LSV techniques. The ionic transference number for the most conducting electrolyte (t_{ion}) is 0.944, with its decomposition potential of 1.6 V. The outcomes confirm the possibility and eligibility of the prepared polymer based electrolyte for energy device applications.

Declaration of Competing Interest

The authors declare that they have no known competing financial interests or personal relationships that could have appeared to influence the work reported in this paper.

Acknowledgements

We would like to acknowledge all support for this work by the University of Sulaimani, University of Human Development, Halabja University and Malaya University. The authors express their gratitude to the support of Princess Nourah bint Abdulrahman University Researchers Supporting Project number (PNURSP2022R58), Princess Nourah bint Abdulrahman University, Riyadh, Saudi Arabia. This work has been supported by Ministry of Higher Education under the Fundamental Research Grant Scheme (FRGS/1/2019/STG07/UM/02/6).

References

Abdulwahid, R.T., Aziz, S.B., Kadir, M.F.Z., 2022. Insights into ion transport in biodegradable solid polymer blend electrolyte based on FTIR analysis and circuit design. J. Phys. Chem. Solids. 167,. https://doi.org/10.1016/j.jpcs.2022.110774 110774.

Agrawal, S.L., Singh, M., Tripathi, M., Dwivedi, M.M., Pandey, K., 2009. Dielectric relaxation studies on [PEO-SiO2]:NH4SCN nanocomposite polymer electrolyte films. J. Mater. Sci. 44, 6060–6068. https://doi.org/10.1007/s10853-009-3833-9.

Ahmed, H.T., Abdullah, O.G., 2020. Structural and ionic conductivity characterization of PEO:MC-NH4I proton-conducting polymer blend electrolytes based films. Results Phys. 16,. https://doi.org/10.1016/j.rinp.2019.102861 102861.

Aniskari, N.A.B., Mohd. Ikmar, N.B.M.I., 2017. The effect of ionic charge carriers in 2-hydroxyethyl cellulose solid biopolymer electrolytes doped glycolic acid via FTIR-deconvolution technique. J. Sustain. Sci. Manage.

Arya, A., Sharma, A.L., 2018. Structural Microstructural and Electrochemical Properties of Dispersed Type Polymer Nanocomposite Films. J. Phys. D. Appl. Phys. 51. https://doi.org/10.1080/14484846.2018.1432089.

Asnawi, A.S.F.M., Aziz, S.B., Nofal, M.M., Yusof, Y.M., Brevik, I., Hamsan, M.H., Brza, M.A., Abdulwahid, R.T., Kadir, M.F.Z., 2020. Metal complex as a novel approach to enhance the amorphous phase and improve the EDLC performance of plasticized proton conducting chitosan-based polymer electrolyte. Membranes (Basel). 10, 1–20. https://doi.org/10.3390/membranes10060132.

Awasthi, P., Das, S., 2019. Reduced electrode polarization at electrode and analyte interface in impedance spectroscopy using carbon paste and paper. Rev. Sci. Instrum. 90. https://doi.org/10.1063/1.5123585.

Aziz, S.B., 2016. Occurrence of electrical percolation threshold and observation of phase transition in chitosan (1–x):AgI x ($0.05 \leq x \leq 0.2$)-based ion-conducting solid polymer composites. Appl. Phys. A Mater. Sci. Process. 122. https://doi.org/10.1007/s00339-016-0235-0.

Aziz, S.B., Brza, M.A., Dannoun, E.M.A., Hamsan, M.H., Hadi, J. M., Kadir, M.F.Z., Abdulwahid, R.T., 2020. The study of electrical and electrochemical properties of magnesium ion conducting CS: PVA based polymer blend electrolytes: Role of lattice energy of magnesium salts on EDLC performance. Molecules 25. https://doi.org/10.3390/molecules25194503.

Aziz, S.B., Ali, F., Anuar, H., Ahamad, T., Kareem, W.O., Brza, M. A., Kadir, M.F.Z., Abu Ali, O.A., Saleh, D.I., Asnawi, A.S.F.M., et al, 2021. Structural and electrochemical studies of proton conducting biopolymer blend electrolytes based on MC: Dextran for EDLC device application with high energy density. Alexandria Eng. J. https://doi.org/10.1016/j.aej.2021.09.026.

Aziz, S.B., Dannoun, E.M.A., Murad, A.R., Mahmoud, K.H., Brza, M.A., Nofal, M.M., Elsayed, K.A., Abdullah, S.N., Hadi, J.M., Kadir, M.F.Z., 2021. Influence of scan rate on CV Pattern: Electrical and electrochemical properties of plasticized Methylcellulose: Dextran (MC:Dex) proton conducting polymer electrolytes. Alexandria Eng. J. https://doi.org/10.1016/j.aej.2021.11.020.

Aziz, S.B., Dannoun, E.M.A., Hamsan, M.H., Ghareeb, H.O., Nofal, M.M., Karim, W.O., Asnawi, A.S.F.M., Hadi, J.M., Kadir, M.F. Z.A., 2021. A polymer blend electrolyte based on cs with enhanced ion transport and electrochemical properties for electrical double layer capacitor applications. Polymers (Basel). 13, 1–18. https://doi.org/10.3390/polym13060930.

Aziz, S.B., Nofal, M.M., Abdulwahid, R.T., Kadir, M.F.Z., Hadi, J. M., Hessien, M.M., Kareem, W.O., Dannoun, E.M.A., Saeed, S. R., 2021. Impedance, FTIR and transport properties of plasticized proton conducting biopolymer electrolyte based on chitosan for electrochemical device application. Results Phys. 29,. https://doi.org/10.1016/j.rinp.2021.104770 104770.

Aziz, S.B., Asnawi, A.S.F.M., Kadir, M.F.Z., Alshehri, S.M., Ahamad, T., Yusof, Y.M., Hadi, J.M., 2021. Structural, electrical and electrochemical properties of glycerolized biopolymers based on chitosan (Cs): Methylcellulose (mc) for energy storage application. Polymers (Basel) 13. https://doi.org/10.3390/polym13081183.

Aziz, S.B., Nofal, M.M., Kadir, M.F.Z., Dannoun, E.M.A., Brza, M. A., Hadi, J.M., Abdulla, R.M., 2021. Bio-Based Plasticized PVA Based Polymer Blend Electrolytes and Electrochemical Properties. Materials (Basel). 14, 1994.

Aziz, S.B., Asnawi, A.S.F.M., Abdulwahid, R.T., Ghareeb, H.O., Alshehri, S.M., Ahamad, T., Hadi, J.M., Kadir, M.F.Z., 2021. Design of potassium ion conducting PVA based polymer electrolyte with improved ion transport properties for EDLC device application. J. Mater. Res. Technol. 13, 933–946. https://doi.org/10.1016/j.jmrt.2021.05.017.

Aziz, S.B., Abdulwahid, R.T., Kadir, M.F., Ghareeb, H.O., Ahamad, T., Alshehri, S.M., 2022. Design of non-faradaic EDLC from plasticized MC based polymer electrolyte with an energy density close to lead-acid batteries. Journal of Industrial and Engineering Chemistry 105, 414–426.

Aziz, NA.N., Idris, N.K., Isa, M.I.N., 2010. Proton conducting polymer electrolytes of methylcellulose doped ammonium fluoride: Conductivity and ionic transport studies. International Journal of Physical Sciences 5 (6), 748–752.

Basha, S.K.S., Sundari, G.S., Kumar, K.V., Rao, M.C., 2018. Preparation and dielectric properties of PVP-based polymer electrolyte films for solid-state battery application. Polym. Bull. 75, 925–945. https://doi.org/10.1007/s00289-017-2072-5.

Brza, M.A., Aziz, S.B., Anuar, H., Ali, F., Abdulwahid, R.T., Hadi, J. M., 2021. Electrochemical Impedance Spectroscopy as a Novel Approach to Investigate the Influence of Metal Complexes on Electrical Properties of Poly(vinyl alcohol) (PVA) Composites. Int. J. Electrochem. Sci. 16, 1–21. https://doi.org/10.20964/2021.05.22.

Brza, M.A., Aziz, S.B., Anuar, H., Alshehri, S.M., Ali, F., Ahamad, T., Hadi, J.M., 2021. Characteristics of a plasticized pva-based polymer electrolyte membrane and h+ conductor for an electrical double-layer capacitor: Structural, morphological, and ion transport properties. Membranes (Basel) 11. https://doi.org/10.3390/membranes11040296.

Castillo, J., Chacón, M., Castillo, R., Vargas, R.A., Bueno, P.R., Varela, J.A., 2009. Dielectric relaxation and dc conductivity on the PVOH-CF3COONH4 polymer system. Ionics (Kiel). 15, 537–544. https://doi.org/10.1007/s11581-009-0320-x.

Chai, M.N., Isa, M.I.N., 2016. Novel Proton Conducting Solid Biopolymer Electrolytes Based on Carboxymethyl Cellulose Doped

with Oleic Acid and Plasticized with Glycerol. Sci. Rep. 6, 1–7. https://doi.org/10.1038/srep27328.

Chai, M.N., Ramlli, M.A., Isa, M.I.N., 2013. Proton conductor of propylene carbonate–plasticized carboxyl methylcellulose–based solid polymer electrolyte. International Journal of Polymer Analysis and Characterization 18 (4), 297–302.

Dannoun, E.M.A., Aziz, S.B., Kadir, M.F.Z., Brza, M.A., Nofal, M. M., Hadi, J.M., Al-Saeedi, S.I., Abdulwahid, R.T., 2022. The Study of Impedance, Ion Transport Properties, EEC Modeling, Dielectric and Electrochemical Characteristics of Plasticized Proton Conducting PVA Based Electrolytes. J. Mater. Res. Technol. 17, 1976–1985. https://doi.org/10.1016/j.jmrt.2022.01.152.

Dave, G., Kanchan, D.K., 2018. Dielectric relaxation and modulus studies of PEO-PAM blend based sodium salt electrolyte system. Indian J. Pure Appl. Phys. 56, 978–988.

Deraman, S.K., Mohamed, N.S., Subban, R.H.Y., 2014. Ionic liquid incorporated pvc based polymer electrolytes: Electrical and dielectric properties. Sains Malaysiana 43, 877–883.

Dueramae, I., Okhawilai, M., Kasemsiri, P., Uyama, H., Kita, R., 2020. Properties enhancement of carboxymethyl cellulose with thermo-responsive polymer as solid polymer electrolyte for zinc ion battery. Sci. Rep. 10, 1–12. https://doi.org/10.1038/s41598-020-69521-x.

Dumitraşcu, M., Albu, M.G., Vîrgolici, M., Vancea, C., Meltzer, V., 2012. Characterization of electron beam irradiated polyvinylpyrrolidone-dextran (PVP/DEX) blends. Solid State Phenom. 188, 102–108. https://doi.org/10.4028/www.scientific.net/SSP.188.102.

Gao, H., Lian, K., 2014. Proton-conducting polymer electrolytes and their applications in solid supercapacitors: A review. RSC Adv. 4, 33091–33113. https://doi.org/10.1039/c4ra05151c.

Hadi, J.M., Aziz, S.B., Mustafa, M.S., Hamsan, M.H., Abdulwahid, R.T., Kadir, M.F.Z., Ghareeb, H.O., 2020. Role of nano-capacitor on dielectric constant enhancement in PEO:NH4SCN:xCeO2 polymer nano-composites: Electrical and electrochemical properties. J. Mater. Res. Technol. 9, 9283–9294. https://doi.org/10.1016/j.jmrt.2020.06.022.

Hadi, J.M., Aziz, S.B., Saeed, S.R., Brza, M.A., Abdulwahid, R.T., Hamsan, M.H., Abdullah, R.M., Kadir, M.F.Z., Muzakir, S.K., 2020. Investigation of ion transport parameters and electrochemical performance of plasticized biocompatible chitosan-based proton conducting polymer composite electrolytes. Membranes (Basel). 10, 1–27. https://doi.org/10.3390/membranes10110363.

Hadi, J.M., Aziz, S.B., Nofal, M.M., Hussen, S.A., Hamsan, M.H., Brza, M.A., Abdulwahid, R.T., Kadir, M.F.Z., Woo, H.J., 2020. Electrical, dielectric property and electrochemical performances of plasticized silver ion-conducting chitosan-based polymer nanocomposites. Membranes (Basel). 10, 1–22. https://doi.org/10.3390/membranes10070151.

Hadi, J.M., Aziz, S.B., Mustafa, M.S., Brza, M.A., Hamsan, M.H., Kadir, M.F.Z., Ghareeb, H.O., Hussein, S.A., 2020. Electrochemical impedance study of proton conducting polymer electrolytes based on PVC doped with thiocyanate and plasticized with glycerol. Int. J. Electrochem. Sci. 15, 4671–4683. https://doi.org/10.20964/2020.05.34.

Hadi, J.M., Aziz, S.B., Kadir, M.F.Z., El-Badry, Y.A., Ahamad, T., Hussein, E.E., Asnawi, A.S.F.M., Abdullah, R.M., Alshehri, S.M., 2021. Design of plasticized proton conducting Chitosan: Dextran based biopolymer blend electrolytes for EDLC application: Structural, impedance and electrochemical studies. Arab. J. Chem. 14,. https://doi.org/10.1016/j.arabjc.2021.103394 103394.

Hadi, J.M., Aziz, S.B., Brza, M.A., Kadir, M.F.Z., Abdulwahid, R.T., Al-Asbahi, B.A., Ahmed, A.A.A., 2022. Structural and energy storage behavior of ion conducting biopolymer blend electrolytes based on methylcellulose: Dextran polymers. Alexandria Engineering Journal 61 (12), 9273–9285.

Hamsan, M.H., Zamani Kadir, M.F., Aziz, S.B., Solihin Azha, M.A., Muzakir, S.K., 2020. Influence of NH4F in Dextran Based Biopolymer Electrolytes: Conductivity and Electrical Analysis. Makara J. Technol. 23, 131. https://doi.org/10.7454/mst.v23i3.3729.

Hamsan, M.H., Shukur, M.F., Aziz, S.B., Kadir, M.F.Z., 2019. Dextran from Leuconostoc mesenteroides-doped ammonium salt-based green polymer electrolyte. Bull. Mater. Sci. 42. https://doi.org/10.1007/s12034-019-1740-5.

Hamsan, M.H., Shukur, M.F., Aziz, S.B., Yusof, Y.M., Kadir, M.F. Z., 2020. Influence of NH 4 Br as an ionic source on the structural/electrical properties of dextran-based biopolymer electrolytes and EDLC application. Bull. Mater. Sci. 43. https://doi.org/10.1007/s12034-019-2008-9.

Iro, Z.S., Subramani, C., Dash, S.S., 2016. A brief review on electrode materials for supercapacitor. Int. J. Electrochem. Sci. 11, 10628–10643. https://doi.org/10.20964/2016.12.50.

Ikmar Nizam Mohamad Isa, M., Amirullah Ramlli, M., Min, I., 2014. Conductivity study of Carboxyl methyl cellulose Solid biopolymer electrolytes (SBE) doped with Ammonium Fluoride FUNDAMENTAL STUDY ON IONIC TRANSPORT OF ENHANCED CMC SOLID BIOPOLYMER ELECTROLYTES VIA FTIR DECONVOLUTION APPROACH View project Conductivity study of Carboxyl methyl cellulose Solid biopolymer electrolytes (SBE) doped with Ammonium Fluoride. Res. J. Recent Sci. 3, 59.

Kadir, M.F.Z. et al, 2018. Biopolymeric electrolyte based on glycerolized methyl cellulose with NH4Br as proton source and potential application in EDLC. Ionics 24 (6), 1651–1662.

Khiar, A.S.A., Puteh, R., Arof, A.K., 2006. Characterizations of chitosan-ammonium triflate (NH 4CF 3so 3) complexes by FTIR and impedance spectroscopy. Phys. Status Solidi Appl. Mater. Sci. 203, 534–543. https://doi.org/10.1002/pssa.200521016.

Kiamahalleh, M.V., Zein, S.H.S., Najafpour, G., Sata, S.A., Buniran, S., 2012. Multiwalled carbon nanotubes based nanocomposites for supercapacitors: A review of electrode materials. Nano 7. https://doi.org/10.1142/S1793292012300022.

Kumar, Y., Pandey, G.P., Hashmi, S.A., 2012. Gel polymer electrolyte based electrical double layer capacitors: Comparative study with multiwalled carbon nanotubes and activated carbon electrodes. J. Phys. Chem. C 116, 26118–26127. https://doi.org/10.1021/jp305128z.

Li, W. et al, 2017. A PEO-based gel polymer electrolyte for lithium ion batteries. RSC advances 7 (38), 23494–23501.

Maheshwari, T., Tamilarasan, K., Selvasekarapandian, S., Chitra, R., Muthukrishnan, M., 2021. Synthesis and characterization of Dextran, poly (vinyl alcohol) blend biopolymer electrolytes with NH4NO3, for electrochemical applications. Int. J. Green Energy 00, 1–17. https://doi.org/10.1080/15435075.2021.1946811.

Malathi, J., Kumaravadivel, M., Brahmanandhan, G.M., Hema, M., Baskaran, R., Selvasekarapandian, S., 2010. Structural, thermal and electrical properties of PVA-LiCF3SO3 polymer electrolyte. J. Non. Cryst. Solids 356, 2277–2281. https://doi.org/10.1016/j.jnoncrysol.2010.08.011.

Mustafa, M.S., Ghareeb, H.O., Aziz, S.B., Brza, M.A., Al-zangana, S., Hadi, J.M., Kadir, M.F.Z., 2020. Electrochemical characteristics of glycerolized PEO-based polymer electrolytes. Membranes (Basel). 10, 1–16. https://doi.org/10.3390/membranes10060116.

Nik Aziz, N.A., Idris, N.K., Isa, M.I.N., 2010. Solid polymer electrolytes based on methylcellulose: FT-IR and ionic conductivity studies. Int. J. Polym. Anal. Charact. 15, 319–327. https://doi.org/10.1080/1023666X.2010.493291.

Nofal, M.M., Aziz, S.B., Hadi, J.M., Abdulwahid, R.T., Dannoun, E. M.A., Marif, A.S., Al-Zangana, S., Zafar, Q., Brza, M.A., Kadir, M.F.Z., 2020. Synthesis of porous proton ion conducting solid polymer blend electrolytes based on PVA: CS polymers: Structural, morphological and electrochemical properties. Materials (Basel). 13, 1–21. https://doi.org/10.3390/ma13214890.

Nofal, M.M., Aziz, S.B., Ghareeb, H.O., Hadi, J.M., Dannoun, E.M. A., Al-Saeedi, S.I., 2022. Impedance and Dielectric Properties of PVC:NH_4I Solid Polymer Electrolytes (SPEs): Steps toward the

Fabrication of SPEs with High Resistivity. Materials. 15 (6), 2143. https://doi.org/10.3390/ma15062143.

Nofal, M.M., Aziz, S.B., Brza, M.A., Abdullah, S.N., Dannoun, E.M. A., Hadi, J.M., Murad, A.R., Al Saeedi, S.I., Kadir, M.F.Z., 2022. Studies of Circuit Design, Structural, Relaxation and Potential Stability of Polymer Blend Electrolyte Membranes Based on PVA: MC Impregnated with NH 4 I. Salt, 1–21.

Nofal, M.M., Hadi, J.M., Aziz, S.B., Brza, M.A., Asnawi, A.S.F.M., Dannoun, E.M.A., Abdullah, A.M., Kadir, M.F.Z., 2021. A study of methylcellulose based polymer electrolyte impregnated with potassium ion conducting carrier: Impedance, eec modeling, ftir, dielectric, and device characteristics. Materials (Basel) 14. https://doi.org/10.3390/ma14174859.

Prajapati, G.K., Roshan, R., Gupta, P.N., 2010. Effect of plasticizer on ionic transport and dielectric properties of PVAH3PO4 proton conducting polymeric electrolytes. J. Phys. Chem. Solids 71, 1717–1723. https://doi.org/10.1016/j.jpcs.2010.08.023.

Pritam, Arya, A., Sharma, A.L., 2020. Selection of best composition of Na+ ion conducting PEO-PEI blend solid polymer electrolyte based on structural, electrical, and dielectric spectroscopic analysis. Ionics (Kiel) 26, 745–766. https://doi.org/10.1007/s11581-019-03245-5.

Ramlli, M.A., Isa, M.I.N., 2016. Structural and ionic transport properties of protonic conducting solid biopolymer electrolytes based on carboxymethyl cellulose doped with ammonium fluoride. J. Phys. Chem. B 120, 11567–11573. https://doi.org/10.1021/acs.jpcb.6b06068.

Rani, M.S.A. et al, 2014. Biopolymer electrolyte based on derivatives of cellulose from kenaf bast fiber. Polymers 6 (9), 2371–2385.

Rauf, H.G., Hadi, J.M., Aziz, S.B., Abdulwahid, R.T., Mustafa, M.S., 2022. A Novel Approach to Design High Resistive Polymer Electrolytes Based on PVC: Electrochemical Impedance and Dielectric Properties. Int. J. Electrochem. Sci 17 (22051), 2.

Shigel, K.I., 2002. Determination of structural peculiarities of dextran, pulluan and gamma irradiated pullulan by Fourier-transform IR spectroscopy. Carbohydr. Res. 337, 2649–2701.

Shuhaimi, N.E.A., Teo, L.P., Majid, S.R., Arof, A.K., 2010. Transport studies of NH4NO3 doped methyl cellulose electrolyte. Synth. Met. 160, 1040–1044. https://doi.org/10.1016/j.synthmet.2010.02.023.

Shuhaimi, N.E.A., Teo, L.P., Woo, H.J., Majid, S.R., Arof, A.K., 2012. Electrical double-layer capacitors with plasticized polymer electrolyte based on methyl cellulose. Polym. Bull. 69, 807–826. https://doi.org/10.1007/s00289-012-0763-5.

Shukur, M.F., Ibrahim, F.M., Majid, N.A., Ithnin, R., Kadir, M.F.Z., 2013. Electrical analysis of amorphous corn starch-based polymer electrolyte membranes doped with LiI. Phys. Scr. 88. https://doi.org/10.1088/0031-8949/88/02/025601.

Shukur, M.F., Kadir, M.F.Z., 2015. Hydrogen ion conducting starch-chitosan blend based electrolyte for application in electrochemical devices. Electrochimica Acta 158, 152–165.

Smaoui, H., Mir, L.E.L., Guermazi, H., Agnel, S., Toureille, A., 2009. Study of dielectric relaxations in zinc oxide-epoxy resin nanocomposites. J. Alloys Compd. 477, 316–321. https://doi.org/10.1016/j.jallcom.2008.10.084.

Sohaimy, M.I.H., Isa, M.I.N., 2017. Ionic conductivity and conduction mechanism studies on cellulose based solid polymer electrolytes doped with ammonium carbonate. Polymer Bulletin 74 (4), 1371–1386.

Turhan, K.N., Sahbaz, F., Güner, A., 2001. A spectrophotometric study of hydrogen bonding in methylcellulose-based edible films plasticized by polyethylene glycol. J. Food Sci. 66, 59–62. https://doi.org/10.1111/j.1365-2621.2001.tb15581.x.

Vettori, M.H.P.B., Franchetti, S.M.M., Contiero, J., 2012. Structural characterization of a new dextran with a low degree of branching produced by Leuconostoc mesenteroides FT045B dextransucrase. Carbohydr. Polym. 88, 1440–1444. https://doi.org/10.1016/j.carbpol.2012.02.048.

Yang, Z., Peng, H., Wang, W., Liu, T., 2010. Crystallization behavior of poly(ε-caprolactone)/layered double hydroxide nanocomposites. J. Appl. Polym. Sci. 116, 2658–2667. https://doi.org/10.1002/app.

Yusof, Y.M. et al, 2014. The effect of plasticization on conductivity and other properties of starch/chitosan blend biopolymer electrolyte incorporated with ammonium iodide. Molecular Crystals and Liquid Crystals 603 (1), 73–88.